

Investigation of neutron transfer in  ${}^7\text{Li} + {}^{124}\text{Sn}$  systemV. V. Parkar<sup>1,2,\*</sup>, A. Parmar,<sup>3</sup> Prasanna M.,<sup>4</sup> V. Jha,<sup>1,2</sup> and S. Kailas<sup>5</sup><sup>1</sup>*Nuclear Physics Division, Bhabha Atomic Research Centre, Mumbai - 400085, India*<sup>2</sup>*Homi Bhabha National Institute, Anushaktinagar, Mumbai - 400094, India*<sup>3</sup>*Sardar Vallabhbhai National Institute of Technology, Surat - 395007, India*<sup>4</sup>*Department of Physics, Rani Channamma University, Belagavi - 591156, India*<sup>5</sup>*UM-DAE Centre for Excellence in Basic Sciences, Mumbai-400098, India*

(Received 23 July 2021; accepted 28 October 2021; published 10 November 2021)

The relative importance of neutron transfer and breakup process in a reaction around Coulomb barrier energies has been studied for the  ${}^7\text{Li} + {}^{124}\text{Sn}$  system. Coupled channel calculations have been performed to understand the one neutron stripping and pickup cross sections along with the breakup in the  ${}^7\text{Li} + {}^{124}\text{Sn}$  system. The systematics of one and two neutron stripping and pickup cross sections with a  ${}^7\text{Li}$  projectile on several targets show an approximate universal behavior, which has been explained by a simple model based on barrier penetration. Complete reaction mechanism have been studied by comparing the reaction cross sections with the measured total fusion and one neutron transfer cross sections.

DOI: [10.1103/PhysRevC.104.054603](https://doi.org/10.1103/PhysRevC.104.054603)

## I. INTRODUCTION

Weakly bound nuclei are characterized by dominant cluster structures and a loose binding with respect to the breakup into these clusters. These features are linked to enhanced cross sections of breakup and transfer channels in reactions involving weakly bound projectiles (WBP) around Coulomb barrier energies. The investigations into the relative importance of different processes on the reaction mechanism is a topic of intense current interest. In this context, several experimental studies have been performed over the years by utilizing projectiles of both stable and unstable weakly bound nuclei. Various processes, such as, elastic scattering, complete and incomplete fusion, inclusive and exclusive breakup, transfer of one or many nucleons, have been studied in reactions around Coulomb barrier energies using WBP [1,2]. In particular, the stable WBPs, such as,  ${}^6\text{Li}$ ,  ${}^7\text{Li}$ , and  ${}^9\text{Be}$  on several targets, have been extensively used for such measurements. Many new features have been highlighted from these studies that were not observed with the strongly bound projectiles (SBP).

From the measurements of elastic scattering, the extracted total reaction cross sections with WBP are found to be much larger than those with comparative SBP [3,4]. Further, a new type of anomaly in the optical potential description of elastic scattering, namely the ‘breakup threshold anomaly’ is observed in the case of WBPs [5], which has been usually attributed to the repulsive polarization potential produced by the cluster breakup process of the projectile [6–8]. In the studies of fusion with WBPs, the complete fusion (CF) cross sections are found to be suppressed at above barrier energies with respect to predictions of one-dimensional barrier

penetration model (1DBPM) [1,2]. An interesting observation in these measurements is that the amount of suppression is commensurate with the measured incomplete fusion (ICF) [9,10]. Total fusion (TF) which is the sum of CF and ICF cross sections match with the 1DBPM predictions at above barrier energies [2]. Large inclusive  $\alpha$ -particle cross sections measured at energies around the Coulomb barrier is another fascinating feature of reactions with WBP [2,11–13]. In the breakup measurements, it was observed that the noncapture breakup (NCBU) was very small compared to the inclusive breakup cross sections [2,14–17]. It has been shown experimentally that the breakup through the indirect path, namely the process consisting of transfer followed by breakup, may provide a dominant contribution [14–16]. However, the neutron transfer to ground state is the dominant process when compared to excited states [15]. Apart from the breakup process that is related to the low  $\alpha$ -binding energies, the importance of neutron transfer has been emphasized for the large production of inclusive  $\alpha$  cross sections [2,18,19]. While many studies have focused on the contribution of the breakup process, the role of neutron transfer has not been investigated well enough. There are not many measurements for the neutron transfer cross section with WBPs and data are scarce [9,13,14,18,20–24].

Due to the availability of the radioactive ion beam (RIB), the features observed in stable WBPs can be explored also for the nuclei away from the line of stability [1,3,25,26]. In these nuclei, besides the low binding energy and cluster structure, there exists a long tail in the density distribution that corresponds to an anomalously large size. This observation may be interpreted in terms of halo and Borromean structures (nuclei comprised of three bound components in which any subsystem of two components is unbound). In many of these nuclei, one or many neutron transfers are found to give quite

\*Corresponding author: [vparkar@barc.gov.in](mailto:vparkar@barc.gov.in)

dominant contribution to the reaction cross section. For example, in the study of  ${}^6\text{Li} + {}^{65}\text{Cu}$ ,  ${}^{197}\text{Au}$  systems, the  $2n$  transfer channel was shown to be dominant [27–29].

On the theoretical front, coupled channel calculations have been successfully utilized for explaining most of the experimental observables and to elucidate on the underlying reaction mechanisms. The continuum discretized coupled channels (CDCC) method [6,7,30–32] has been used to study the breakup process by including the couplings to the continuum states above the breakup threshold of the projectile nucleus. Using this method, both the one-step process of continuum excitation called prompt breakup and the two-step process of excitation of long-lived resonances in the continuum followed by decay, namely the delayed breakup, are taken into account. The transfer processes are described through the coupled reaction channel (CRC) calculations that involves the multistate couplings in the projectile and target like nucleus before and after the transfer of the nucleon(s).

While the systematics of the fusion and elastic scattering have been studied well, the systematic studies of the available data of neutron transfer have not been performed. In the present work, we study the one-neutron stripping and pickup cross sections in the  ${}^7\text{Li} + {}^{124}\text{Sn}$  reaction and investigate the relative importance of the breakup and transfer processes through the CDCC and CRC calculations. The systematics of neutron transfer cross sections for different targets is also studied. The paper is organized as follows. Calculation details are given in Sec. II. The results are discussed in Sec. III and a summary is given in Sec. IV.

## II. CALCULATION DETAILS

To understand the mechanism of transfer and breakup reactions, coupled channel calculations have been performed. We have performed three kinds of calculations: (i) CRC using global phenomenological optical model potentials, (ii) CRC using normalized microscopic São Paulo potentials, (iii) CDCC, and (iv) combined CDCC+CRC. All these calculations have been performed using the code FRESKO (version FRES 2.9) [33]. Next, we discuss about the calculation methods for each case in detail.

### A. CRC calculations

In these types of calculations, optical model potentials for entrance and exit channels are required. Apart from this, binding potentials of the fragment and core for the projectile and target partitions are required. The potentials binding the transferred particles were of Woods-Saxon volume form with radius  $1.25A^{1/3}$  fm and diffuseness 0.65 fm, with ‘A’ being the mass of the core nucleus. The depths were adjusted to obtain the required binding energies of the particle-core composite system. The single particle states along with spectroscopic factors ( $C^2S$ ) considered in the calculations are given in Table I. For the  ${}^7\text{Li} \rightarrow {}^6\text{Li} + n$  transfer, both the  $1p_{3/2}$  and  $1p_{1/2}$  components of the neutron bound to  ${}^6\text{Li}$  were included with spectroscopic factors of  $C^2S = 0.43$  and  $0.29$ , respectively [34,35], taken from Cohen and Kurath [36]. Similarly for  ${}^7\text{Li} + n \rightarrow {}^8\text{Li}$  transfer, both the  $1p_{3/2}$  and  $1p_{1/2}$  com-

TABLE I. Energy levels of residual nuclei and spectroscopic factors ( $C^2S$ ) used for neutron transfer channels:  ${}^{124}\text{Sn} \rightarrow {}^{125}\text{Sn}$  [54] and  ${}^{124}\text{Sn} \rightarrow {}^{123}\text{Sn}$  [55].

${}^{125}\text{Sn}$			${}^{123}\text{Sn}$		
$E$ (MeV)	$J^\pi$	$C^2S$	$E$ (MeV)	$J^\pi$	$C^2S$
0.000	$11/2^-$	0.42	0.000	$11/2^-$	4.49
0.026	$3/2^+$	0.44	0.025	$3/2^+$	4.49
0.232	$1/2^+$	0.33	0.139	$1/2^+$	1.90
0.930	$7/2^-$	0.015	0.920	$3/2^+$	1.00
1.277	$5/2^+$	0.07	1.028	$7/2^+$	2.79
1.377	$7/2^+$	0.038	1.155	$7/2^+$	3.20
1.555	$5/2^+$	0.040	1.194	$5/2^+$	1.00
2.264	$5/2^+$	0.019	1.484	$5/2^+$	2.79
2.600	$7/2^-$	0.010	1.784	$5/2^+$	1.00
2.767	$7/2^-$	0.54	1.902	$5/2^+$	1.00
2.890	$7/2^-$	0.032	2.026	$5/2^+$	1.00
3.016	$7/2^-$	0.040	2.365	$7/2^+$	1.00
3.085	$7/2^-$	0.040	2.446	$1/2^+$	1.00
			2.850	$5/2^+$	1.00
			3.152	$7/2^-$	1.00

ponents of the neutron bound to  ${}^7\text{Li}$  were included with spectroscopic factors of  $C^2S = 0.98$  and  $0.056$ , respectively [34], taken from Cohen and Kurath [36]. The finite range form factors in the post form for stripping and prior form for pickup were used. Calculations were carried out including the full complex remnant term. In the following subsections, we discuss calculations using global phenomenological optical model potentials and microscopic double folding model potentials.

#### 1. CRC calculations using global phenomenological optical model potentials

Recently, the global phenomenological optical model potentials for  ${}^6\text{Li}$ ,  ${}^7\text{Li}$ , and  ${}^8\text{Li}$  have been proposed [37–39] which have been used for entrance  ${}^7\text{Li} + {}^{124}\text{Sn}$  and exit  ${}^6\text{Li} + {}^{125}\text{Sn}$  (for stripping) and  ${}^8\text{Li} + {}^{123}\text{Sn}$  (for pickup) channels. We refer the results of these calculations as CRC1. The potential parameters are listed in Table II. The old set of global phenomenological optical model potentials for  ${}^{6,7}\text{Li}$  of Cook *et al.* [35] have also been tried for comparison and the results have been found to be the similar.

#### 2. CRC calculations using São Paulo potentials

The calculations have also been performed using microscopic double-folding São Paulo potentials [41,42] for real and imaginary parts of the optical potential. At near barrier energies, this potential is equivalent to the usual double folding potential with the advantage that it has a comprehensive systematic for the matter densities. For this reason, this can be considered as a parameter-free potential. Since the breakup channel was not considered explicitly in CRC calculations, the strength coefficients for real and imaginary potentials were kept as  $N_R = N_I = 0.6$ . A similar method was adopted in Refs. [6,20,21,43,44] to account for the loss of flux to dis-

TABLE II. Optical model potential parameters used in CRC calculations. The radius parameter in the potentials are derived from  $R_i = r_i A^{1/3}$ , where  $i = R, V, S, C$  and  $A$  is the target mass number.

System	$V_R$ (MeV)	$r_R$ (fm)	$a_R$ (fm)	$W_V$ (MeV)	$r_V$ (fm)	$a_V$ (fm)	$W_S$ (MeV)	$r_S$ (fm)	$a_S$ (fm)	$r_C$ (fm)	Ref.
$^7\text{Li} + ^{124}\text{Sn}$	179.9	1.24	0.85	22.22	1.59	0.60	36.01	1.18	0.87	1.80	[38]
$^6\text{Li} + ^{125}\text{Sn}$	259.2	1.12	0.81	0.49	1.54	0.73	25.29	1.31	0.94	1.67	[37]
$^8\text{Li} + ^{123}\text{Sn}$	171.2	1.23	0.79	24.43	1.80	0.53	29.19	1.46	0.92	1.57	[39]
$^8\text{Be} + ^{123}\text{In}$	261.4	1.34	0.73	12.12	1.64	0.60	48.15	1.20	0.84	1.56	[40]

sipative and breakup channels [43,44] and repulsive nature of the real part of the breakup polarization potential [6–8,45–49]. In the outgoing partition, the São Paulo potential was used for both the real and the imaginary parts with strength coefficients  $N_R = 1.0$  and  $N_I = 0.78$ . This procedure has been shown to be suitable for describing the elastic scattering cross section for many systems in a wide energy interval [50]. We refer to the results of these calculations as CRC2.

### B. CDCC and CDCC+CRC calculations

To investigate the effect of projectile breakup and neutron transfer on elastic scattering simultaneously, the CDCC and combined CDCC + CRC calculations have been carried out. Both the inelastic (bound and unbound) excitations of the projectile and neutron transfer channels have been coupled.

The coupling scheme used in CDCC is similar to that described in earlier works [51,52]. The calculations assumed a two-body  $\alpha$ - $t$  cluster structure for the  $^7\text{Li}$  nucleus. The ground state and inelastic excitation of  $^7\text{Li}$  were considered as pure  $L = 1$  cluster states, where  $L$  is the relative angular momentum of clusters. The continuum above the  $^7\text{Li} \rightarrow \alpha + t$  breakup threshold (2.47 MeV) was discretized into bins of constant momentum width  $k = 0.20 \text{ fm}^{-1}$ , where  $\hbar k$  is the momentum of  $\alpha + t$  relative motion. The binding potentials for all the bound and continuum cluster states were the well-known potentials from Ref. [53]. The cluster wave functions for each bin in the continuum were averaged over the bin width and each of these bins was then treated as an excited state of  $^7\text{Li}$  with an excitation energy equal to the mean of the bin energy range. The continuum momentum bins were truncated at the upper limits of  $k_{\text{max}} = 0.8 \text{ fm}^{-1}$  for the calculations. The continuum states with relative orbital angular momentum  $L = 0, 1, 2$ , and  $3$  were included. In addition the full continuum continuum (CC) couplings were taken into account in the final calculations. The real part of required fragment-target potentials  $V_{\alpha-T}$  and  $V_{t-T}$  in cluster folding model were taken from São Paulo potential [42], while short range imaginary potential with values  $W_0 = 25 \text{ MeV}$ ,  $r_w = 1.00 \text{ fm}$ ,  $a_w = 0.40 \text{ fm}$  was used. In addition to CDCC calculations for breakup, the CRC calculations of type CRC1 as explained above were simultaneously performed.

## III. RESULTS AND DISCUSSION

### A. Elastic scattering

The elastic scattering data available for the  $^7\text{Li} + ^{120}\text{Sn}$  system at 20, 22, 24, 26, 28, and 30 MeV [56,57] and

for the  $^7\text{Li} + ^{124}\text{Sn}$  system at 28 MeV [58] were utilized for testing our entrance channel potentials and also to see the effect of breakup and neutron transfer couplings on the elastic scattering angular distributions. It is to be noted that the measured elastic scattering angular distributions with the  $^7\text{Li}$  projectile on  $^{120}\text{Sn}$  and  $^{124}\text{Sn}$  targets at 28 MeV are similar as shown in Fig. 1. The calculations of CRC2 type along with CDCC and CDCC+CRC are shown with the data in Fig. 1. Dotted lines are the calculations with bare potential without including any continuum couplings. The coupling effects are evident at above barrier energies. Around the barrier (20 and 22 MeV), the coupling effects are negligible.

To understand the coupling effects for the elastic scattering angular distribution in a better way, we have investigated the behavior of the dynamic polarization potential (DPP) generated due to these couplings. In general, DPP is complex, nonlocal, energy and angular momentum dependent. The complex,  $L$ -dependent polarization potentials are obtained by solving single-channel Schrödinger equation with an effective potential which is comprised of bare potential and polariza-

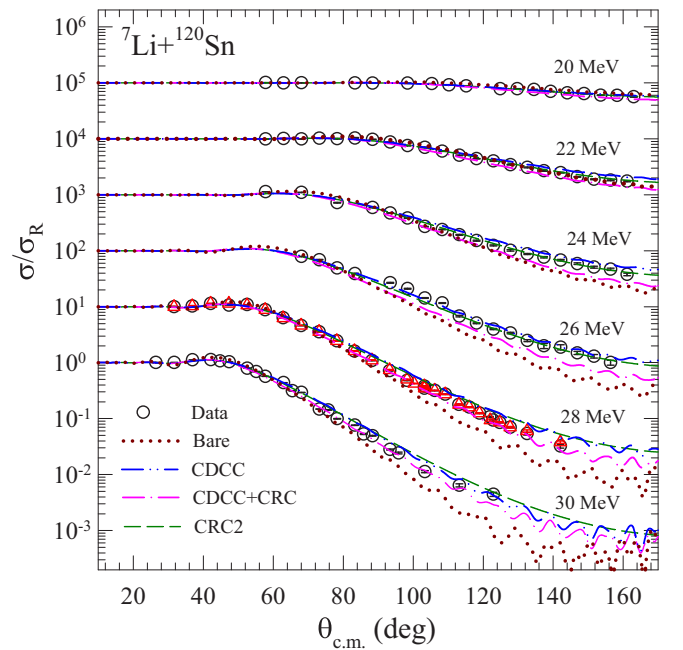


FIG. 1. Elastic scattering data for the  $^7\text{Li} + ^{120}\text{Sn}$  system [56,57] are compared with the calculations. Red triangle data are for the  $^7\text{Li} + ^{124}\text{Sn}$  system [58] at 28 MeV (see text for details).

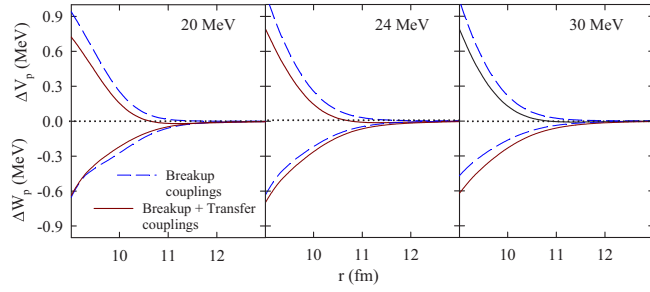


FIG. 2. Real and imaginary parts of dynamic polarization potentials due to breakup (dashed lines) and breakup+transfer (solid lines) couplings in the  ${}^7\text{Li} + {}^{124}\text{Sn}$  system at three bombarding energies 20, 24, and 30 MeV.

tion potential generated due to couplings [59]. This trivially equivalent  $L$ -dependent polarization potential (TELP) is defined as

$$V_L^P(r) = \frac{1}{u_L(r)} \langle V \hat{O} V_{u_L} \rangle_r \quad (1)$$

The DPP in FRESKO is derived as an  $L$ -independent weighted mean local potential from TELP [60] with the weights proportional to the calculated partial reaction cross-sections as given below:

$$V^P(r) = \frac{\sum_L \omega_L(r) V_L^P(r)}{\sum_L \omega_L(r)}, \quad (2)$$

where  $\omega_L(r)$  are weight factors chosen as

$$\omega_L(r) = a_L |u_L(r)|^2 \quad (3)$$

with  $a_L \propto \sigma_R(L)$  (partial reaction cross section).

The calculated DPPs due to breakup (CDCC calculation) and transfer and breakup together (CDCC+CRC calculations) couplings in the vicinity of the strong absorption radii are shown for three (20, 24, and 30 MeV) energies in Fig. 2. It is evident from Fig. 2 that the breakup couplings give rise to repulsive real and attractive imaginary DPPs. After inclusion of transfer couplings, the real part of DPP is slightly reduced. Similar behavior was also observed in the reaction with  ${}^9\text{Be}$  projectile [49,61].

### B. $1n$ stripping, $1n$ pickup, and $1p$ pickup

The  $1n$  stripping data leading to  ${}^{125}\text{Sn}$  residual nucleus was measured by offline  $\gamma$ -ray counting and reported in Ref. [9]. The ground state  $Q$  value for  $n$  stripping for this reaction is  $-1.52$  MeV. The calculations of CRC (CRC1, CRC2) and CDCC+CRC type are compared with the measured data in Fig. 3. A reasonable agreement between the data and calculations imply that the states in  ${}^{125}\text{Sn}$  residual nucleus up to 3 MeV (given in Table I) that were included in the calculations are sufficient to explain the measured data. Contribution from the states higher than 3 MeV or other indirect paths do not have a significant role in the description of experimental data. Similar to  $1n$  stripping channel, the data for  $1n$  pickup leading to  ${}^{123}\text{Sn}$  residual nucleus [only metastable state (m.s.)] was also measured in Ref. [9]. The ground state  $Q$  value for  $n$  pickup for this reaction is  $-6.46$  MeV. The calculations of

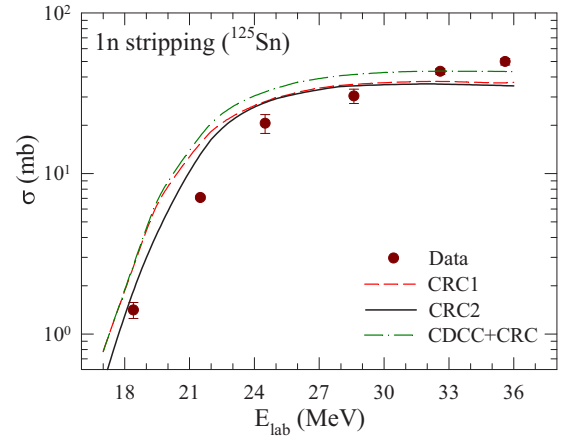


FIG. 3. Measured one neutron stripping cross sections in the  ${}^7\text{Li} + {}^{124}\text{Sn}$  system are compared with the three set of calculations (see text for details).

CRC (CRC1, CRC2) and CDCC+CRC type are compared with the measured data in Fig. 4. The calculations show a large underprediction as compared to the data. The states in  ${}^{123}\text{Sn}$  residual nucleus up to 3 MeV (given in Table I) were coupled. The states above 3 MeV were not measured in the literature [62]. Also, the spectroscopic information about only a few states having large spectroscopic factors is available in the literature [55].

The  ${}^{123}\text{Sn}$  residual nucleus may have a contribution from  $1p$  pickup also. The ground state  $Q$  value for  $p$  pickup for this reaction is  $+5.16$  MeV.  $1p$  pickup will populate  ${}^{123}\text{In}$  which again decays to  ${}^{123}\text{Sn}$ . Hence, the measured  ${}^{123}\text{Sn}$  will have a contribution from both  $1p$  pickup and  $1n$  pickup. We have done CRC1 calculation for  $1p$  pickup considering  ${}^8\text{Be} + {}^{123}\text{In}$  in the exit channel. The  ${}^{123}\text{In}$  states with known spectroscopic factors [62] along with  ${}^8\text{Be}$  g.s.( $0^+$ ) and first excited state ( $3.03$  MeV,  $2^+$ ) have been used. The calculations are shown

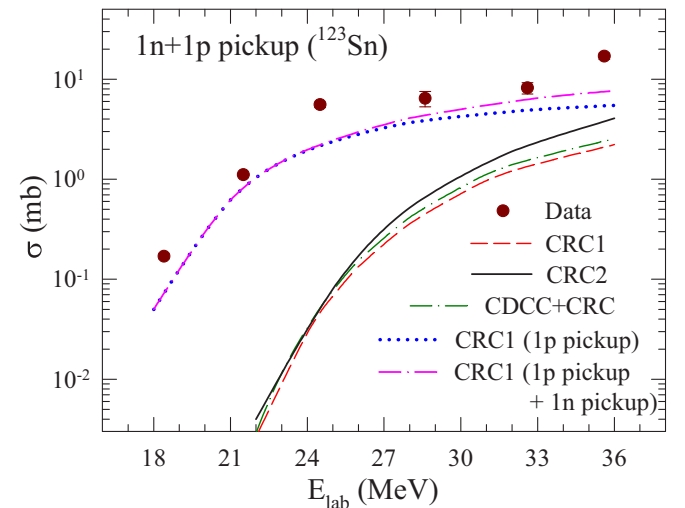


FIG. 4. Measured combined one neutron and one proton pickup cross sections in the  ${}^7\text{Li} + {}^{124}\text{Sn}$  system are compared with the calculations (see text for details).



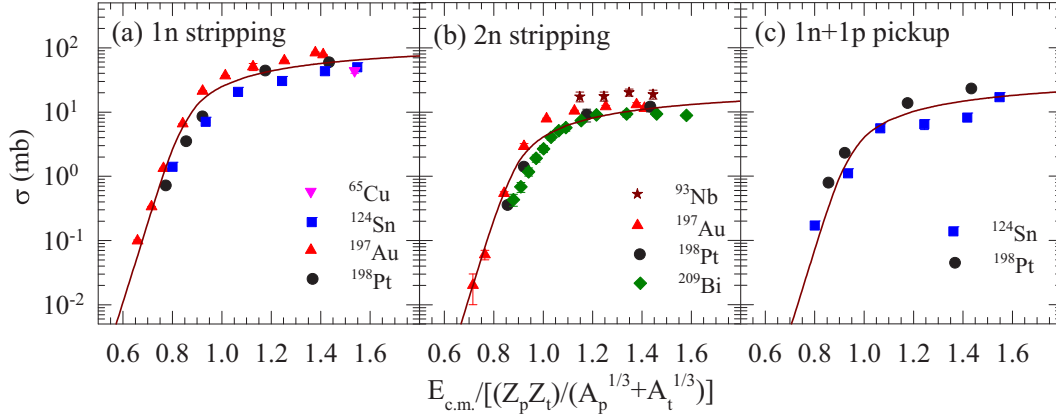


FIG. 5. Systematic behavior of (a) one neutron stripping, (b) two neutron stripping, and (c) combined one neutron and one proton pickup cross sections as a function of reduced energy with  ${}^7\text{Li}$  projectile on various targets. Lines are fit to the data.

in Fig. 4 as CRC1 ( $1p$  pickup), which is found to be much more than  $1n$  pickup. The addition of  $1n$  pickup and  $1p$  pickup cross sections is also shown which is in good agreement with the data.

### C. Systematics of transfer cross sections with ${}^7\text{Li}$ projectile

The data available for  $1n$  stripping,  $2n$  stripping, and  $1n$  pickup cross sections with  ${}^7\text{Li}$  projectile on  ${}^{65}\text{Cu}$  [14],  ${}^{93}\text{Nb}$  [13],  ${}^{124}\text{Sn}$  [9],  ${}^{197}\text{Au}$  [23],  ${}^{198}\text{Pt}$  [24], and  ${}^{209}\text{Bi}$  [63] targets are plotted in Fig. 5(a)–5(c). The variable on the x axis is chosen so as to remove any geometrical factors due to target size. As can be seen from the figure, universal behavior in the cross sections in all three plots is observed. Here, we want to point out that the reported  $1n$  pickup cross sections in  ${}^{124}\text{Sn}$  [9] and  ${}^{198}\text{Pt}$  [24] are actually combined  $1n$  pickup and  $1p$  pickup cross sections.  $1p$  pickup in the  ${}^7\text{Li} + {}^{124}\text{Sn}$  system will populate  ${}^{123}\text{In}$  which will decay to  ${}^{123}\text{Sn}$ . Similarly,  $1p$  pickup in the  ${}^7\text{Li} + {}^{198}\text{Pt}$  system will populate  ${}^{197}\text{Ir}$ , which will decay to  ${}^{197}\text{Pt}$ . The transfer systematics in Fig. 5(a)–5(c) are interesting and it is the first time that these systematics have been presented with the  ${}^7\text{Li}$  projectile. With the  ${}^9\text{Be}$  projectile, a similar universal behavior in neutron stripping cross sections was observed [21]. In addition, a similar universal behavior was also shown earlier for the inclusive  $\alpha$  [2,12,13], triton capture [13], fusion [2], and reaction [3] cross sections. In order to explain the appearance of universal barrier in these plots [Fig. 5(a)–5(c)], we have used the Wong formula [64] that is based on the barrier penetration. The expression of the Wong formula has been modified and multiplied by transfer probability [ $\exp(-cS_{n/2n})$ ] as given below

$$\sigma = \frac{\hbar\omega}{2E_{c.m.}} R_b^2 \log \left[ 1 + \exp \left( \frac{2\pi}{\hbar\omega} (E_{c.m.} - V_b - a) \right) \right] \times \exp(-cS_{n/2n}), \quad (4)$$

where  $a$  and  $c$  are the parameters which were varied to fit the data.  $S_n$  and  $S_{2n}$  are the separation energies for  $1n$  stripping and/or pickup and for  $2n$  stripping, respectively. Parameter ‘ $a$ ’ represents the shift in the barrier for the specific reaction channel while parameter ‘ $c$ ’ provides the overall normalization to describe the transfer cross section in magnitude. The

values of  $V_b$ ,  $R_b$  and  $\hbar\omega$  for the  ${}^7\text{Li} + {}^{124}\text{Sn}$  system were taken from Ref. [9]. The resulting fits are shown as the solid lines in Fig. 5(a)–5(c). The values of  $a$  and  $c$  that have been obtained are given in Table III. The values of parameter ‘ $a$ ’ explains the early onset of these transfer processes as compared to the nominal barrier as observed in data.

### D. Reaction mechanism in the ${}^7\text{Li} + {}^{124}\text{Sn}$ system

To understand the complete reaction mechanism in the  ${}^7\text{Li} + {}^{124}\text{Sn}$  system, the measured CF, ICF, neutron transfer cross sections [9], and their sum are compared with the deduced reaction cross sections from the present calculations, shown in Fig. 6. It also shows the fusion cross sections calculated in CDCC by the barrier penetration model (BPM) using the bare potential. In the BPM, the fusion cross section is calculated from the barrier penetration coefficients,  $T_l$ , using the following relation [65]:

$$\sigma_{\text{fus}} = \frac{\pi}{K^2} \sum_{\ell} (2\ell + 1) T_{\ell}. \quad (5)$$

The coefficients  $T_l$  in turn are calculated using the WKB approximation and they depend on the Coulomb barrier,  $U_B = U_{\text{nuclear}}^{\text{real}} + U_{\text{Coulomb}}$ . BPM fusion cross sections reproduces the experimental TF at above barrier energies while underpredict it at sub-barrier energies, as also observed in Ref. [48]. The cumulative absorption cross sections from CDCC+CRC calculations are found to agree with the cumulative TF and transfer cross sections. NCBU cross sections from CDCC calculations are also shown, which have lower contributions compared to CF, ICF, and  $1n$  stripping. As we have not in-

TABLE III.  $a$  and  $c$  values obtained from the fitting of universal plots of Fig. 5.

Process	$S_{n/2n}$ (MeV)	$a$ (MeV)	$c$ (MeV $^{-1}$ )
(a) $1n$ stripping	7.25	−3.58	0.44
(b) $2n$ stripping	12.92	−2.86	0.37
(c) $1n + 1p$ pickup	2.03	−1.86	2.16

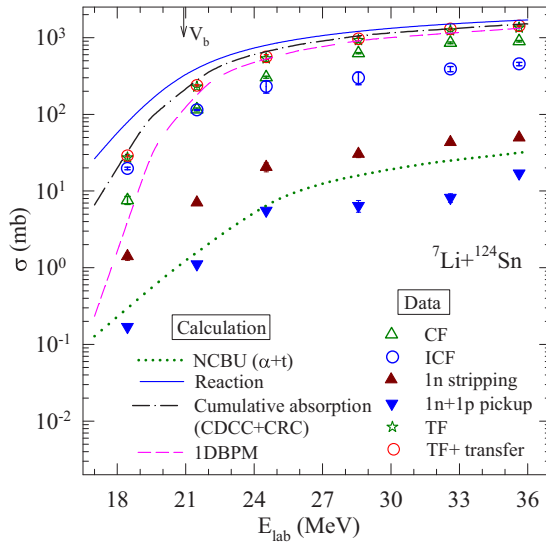


FIG. 6. Measured CF, ICF, transfer cross sections [9] and their sum are compared with the reaction cross sections. NCBU, cumulative absorption, and BPM model calculations are also shown (see text for details).

cluded (not measured) the inelastic excitations, NCBU, and remaining transfer channels, the reaction cross sections are larger than the sum of TF and transfer cross sections.

#### IV. SUMMARY

In summary, we have investigated the important underlying reaction mechanisms, namely breakup and neutron transfer

for the  ${}^7\text{Li} + {}^{124}\text{Sn}$  system around the Coulomb barrier energies. These processes are found to affect the elastic scattering and the fusion cross sections. We have performed the CRC calculations using the global optical model potential parameters as well as using the São Paulo potential for the  ${}^7\text{Li} + {}^{124}\text{Sn}$  system to investigate the role of neutron transfer processes. Since breakup plays an important role for the WBP, we have performed CDCC+CRC calculations to take into account the combined effects of breakup and transfer channels. These calculations provide a simultaneous description of elastic scattering,  $1n$  stripping, combined  $1n$  and  $1p$  pickup and total fusion processes. One of the important findings of this work is the explanation of the observed universal behavior of stripping and pickup cross sections with  ${}^7\text{Li}$  projectile on several targets in terms of a simple phenomenological model. An early onset of the neutron transfer compared to fusion reactions is seen. It is observed that while  $1n$  stripping contributes significantly, other reaction channels, such as, proton stripping, noncapture breakup and target inelastic states might be necessary for a complete description of the reaction cross section for the  ${}^7\text{Li} + {}^{124}\text{Sn}$  system.

#### ACKNOWLEDGMENTS

The authors V.V.P. and S.K. acknowledge the financial support from Young Scientist Research grant and Senior Scientist programme, respectively, from the Indian National Science Academy (INSA), Government of India, in carrying out these investigations.

- [1] L. F. Canto, P. R. S. Gomes, R. Donangelo, J. Lubian, and M. S. Hussein, *Phys. Rep.* **596**, 1 (2015), and references therein.
- [2] V. Jha, V. V. Parkar, and S. Kailas, *Phys. Rep.* **845**, 1 (2020), and references therein.
- [3] J. J. Kolata, V. Guimarães, and E. F. Aguilera, *Eur. Phys. J. A* **52**, 123 (2016).
- [4] E. F. Aguilera, I. Martel, A. M. Sánchez-Benítez, and L. Acosta, *Phys. Rev. C* **83**, 021601(R) (2011).
- [5] H. Kumawat, C. Joshi, V. V. Parkar, V. Jha, B. J. Roy, Y. S. Sawant, P. C. Rout, E. T. Mirgule, R. K. Singh, N. L. Singh *et al.*, *Nucl. Phys. A* **1002**, 121973 (2020).
- [6] Y. Sakuragi, M. Yahiro, and M. Kamimura, *Prog. Theor. Phys.* **70**, 1047 (1983).
- [7] M. Kamimura, M. Yahiro, Y. Iseri, Y. Sakuragi, H. Kameyama, and M. Kawai, *Prog. Theor. Phys. Suppl.* **89**, 1 (1986).
- [8] Y. Sakuragi, *Phys. Rev. C* **35**, 2161 (1987).
- [9] V. V. Parkar, S. K. Sharma, R. Palit, S. Upadhyaya, A. Shrivastava, S. K. Pandit, K. Mahata, V. Jha, S. Santra, K. Ramachandran, T. N. Nag, P. K. Rath, B. Kanagalekar, and T. Trivedi, *Phys. Rev. C* **97**, 014607 (2018).
- [10] V. V. Parkar, S. K. Pandit, A. Shrivastava, R. Palit, K. Mahata, V. Jha, K. Ramachandran, S. Gupta, S. Santra, S. K. Sharma, S. Upadhyaya, T. N. Nag, S. Bhattacharya, T. Trivedi, and S. Kailas, *Phys. Rev. C* **98**, 014601 (2018).
- [11] H. Kumawat, V. Jha, V. V. Parkar, B. J. Roy, S. Santra, V. Kumar, D. Dutta, P. Shukla, L. M. Pant, A. K. Mohanty, R. K. Choudhury, and S. Kailas, *Phys. Rev. C* **81**, 054601 (2010).
- [12] S. Santra, S. Kailas, V. V. Parkar, K. Ramachandran, V. Jha, A. Chatterjee, P. K. Rath, and A. Parihari, *Phys. Rev. C* **85**, 014612 (2012).
- [13] S. K. Pandit, A. Shrivastava, K. Mahata, V. V. Parkar, R. Palit, N. Keeley, P. C. Rout, A. Kumar, K. Ramachandran, S. Bhattacharyya, V. Nanal, C. S. Palshetkar, T. N. Nag, S. Gupta, S. Biswas, S. Saha, J. Sethi, P. Singh, A. Chatterjee, and S. Kailas, *Phys. Rev. C* **96**, 044616 (2017).
- [14] A. Shrivastava, A. Navin, N. Keeley, K. Mahata, K. Ramachandran, V. Nanal, V. V. Parkar, A. Chatterjee, and S. Kailas, *Phys. Lett. B* **633**, 463 (2006).
- [15] S. K. Pandit, A. Shrivastava, K. Mahata, N. Keeley, V. V. Parkar, P. C. Rout, K. Ramachandran, I. Martel, C. S. Palshetkar, A. Kumar, A. Chatterjee, and S. Kailas, *Phys. Rev. C* **93**, 061602(R) (2016).
- [16] D. Chattopadhyay, S. Santra, A. Pal, A. Kundu, K. Ramachandran, R. Tripathi, B. J. Roy, T. N. Nag, Y. Sawant, B. K. Nayak, A. Saxena, and S. Kailas, *Phys. Rev. C* **97**, 051601(R) (2018).
- [17] D. Chattopadhyay, S. Santra, A. Pal, A. Kundu, K. Ramachandran, R. Tripathi, D. Sarkar, S. Sodaye, B. K. Nayak, A. Saxena, and S. Kailas, *Phys. Rev. C* **94**, 061602(R) (2016).
- [18] M. K. Pradhan, A. Mukherjee, Subinit Roy, P. Basu, A. Goswami, R. Kshetri, R. Palit, V. V. Parkar, M. Ray, M. Saha Sarkar, and S. Santra, *Phys. Rev. C* **88**, 064603 (2013).
- [19] V. V. Parkar, V. Jha, and S. Kailas (unpublished) (2021).

- [20] S. P. Hu, G. L. Zhang, J. C. Yang, H. Q. Zhang, P. R. S. Gomes, J. Lubian, J. L. Ferreira, X. G. Wu, J. Zhong, C. Y. He, Y. Zheng, C. B. Li, G. S. Li, W. W. Qu, F. Wang, L. Zheng, L. Yu, Q. M. Chen, P. W. Luo, H. W. Li, Y. H. Wu, W. K. Zhou, B. J. Zhu, and H. B. Sun, *Phys. Rev. C* **93**, 014621 (2016).
- [21] Y. D. Fang, P. R. S. Gomes, J. Lubian, J. L. Ferreira, D. R. Mendes Junior, X. H. Zhou, M. L. Liu, N. T. Zhang, Y. H. Zhang, G. S. Li, J. G. Wang, S. Guo, Y. H. Qiang, B. S. Gao, Y. Zheng, X. G. Lei, and Z. G. Wang, *Phys. Rev. C* **93**, 034615 (2016).
- [22] G. L. Zhang, G. X. Zhang, S. P. Hu, Y. J. Yao, J. B. Xiang, H. Q. Zhang, J. Lubian, J. L. Ferreira, B. Paes, E. N. Cardozo, H. B. Sun, J. J. Valiente-Dobon, D. Testov, A. Goasduff, P. R. John, M. Siciliano, F. Galtarossa, R. Francesco, D. Mengoni, D. Bazzacco, E. T. Li, X. Hao, and W. W. Qu, *Phys. Rev. C* **97**, 014611 (2018).
- [23] C. S. Palshetkar, S. Thakur, V. Nanal, A. Shrivastava, N. Dokania, V. Singh, V. V. Parkar, P. C. Rout, R. Palit, R. G. Pillay, S. Bhattacharyya, A. Chatterjee, S. Santra, K. Ramachandran, and N. L. Singh, *Phys. Rev. C* **89**, 024607 (2014).
- [24] A. Shrivastava, A. Navin, A. Diaz-Torres, V. Nanal, K. Ramachandran, M. Rejmund, S. Bhattacharyya, A. Chatterjee, S. Kailas, A. Lemasson *et al.*, *Phys. Lett. B* **718**, 931 (2013).
- [25] N. Keeley, N. Alamanos, K. W. Kemper, and K. Rusek, *Prog. Part. Nucl. Phys.* **63**, 396 (2009).
- [26] N. Keeley, R. Raabe, N. Alamanos, and J. L. Sida, *Prog. Part. Nucl. Phys.* **59**, 579 (2007).
- [27] A. Chatterjee, A. Navin, A. Shrivastava, S. Bhattacharyya, M. Rejmund, N. Keeley, V. Nanal, J. Nyberg, R. G. Pillay, K. Ramachandran, I. Stefan, D. Bazin, D. Beaumel, Y. Blumenfeld, G. de France, D. Gupta, M. Labiche, A. Lemasson, R. Lemmon, R. Raabe, J. A. Scarpaci, C. Simenel, and C. Timis, *Phys. Rev. Lett.* **101**, 032701 (2008).
- [28] A. Lemasson, A. Navin, N. Keeley, M. Rejmund, S. Bhattacharyya, A. Shrivastava, D. Bazin, D. Beaumel, Y. Blumenfeld, A. Chatterjee, D. Gupta, G. de France, B. Jacquot, M. Labiche, R. Lemmon, V. Nanal, J. Nyberg, R. G. Pillay, R. Raabe, K. Ramachandran, J. A. Scarpaci, C. Simenel, I. Stefan, and C. N. Timis, *Phys. Rev. C* **82**, 044617 (2010).
- [29] A. Lemasson, A. Navin, M. Rejmund, N. Keeley, V. Zelevinsky, S. Bhattacharyya, A. Shrivastava, D. Bazin, D. Beaumel, Y. Blumenfeld *et al.*, *Phys. Lett. B* **697**, 454 (2011).
- [30] M. Yahiro, M. Nakano, Y. Iseri, and M. Kamimura, *Prog. Theor. Phys.* **67**, 1467 (1982).
- [31] Y. Sakuragi, M. Yahiro, and M. Kamimura, *Prog. Theor. Phys. Suppl.* **89**, 136 (1986).
- [32] N. Austern, Y. Iseri, M. Kamimura, M. Kawai, G. Rawitscher, and M. Yahiro, *Phys. Rep.* **154**, 125 (1987).
- [33] Ian J. Thompson, *Comput. Phys. Rep.* **7**, 167 (1988).
- [34] P. Schumacher, N. Ueta, H. H. Duhm, K. I. Kubo, and W. J. Klages, *Nucl. Phys. A* **212**, 573 (1973).
- [35] J. Cook, *Nucl. Phys. A* **388**, 153 (1982).
- [36] S. Cohen and D. Kurath, *Nucl. Phys. A* **101**, 1 (1967).
- [37] Y. Xu, Y. Han, J. Hu, H. Liang, Z. Wu, H. Guo, and C. Cai, *Phys. Rev. C* **98**, 024619 (2018).
- [38] Y. Xu, Y. Han, J. Hu, H. Liang, Z. Wu, H. Guo, and C. Cai, *Phys. Rev. C* **97**, 014615 (2018).
- [39] X. W. Su, Y. L. Han, H. Y. Liang, Z. D. Wu, H. R. Guo, and C. H. Cai, *Phys. Rev. C* **95**, 054606 (2017).
- [40] Y. Xu, Y. Han, H. Liang, Z. Wu, H. Guo, and C. Cai, *Phys. Rev. C* **99**, 034618 (2019).
- [41] L. C. Chamon, D. Pereira, M. S. Hussein, M. A. Cândido Ribeiro, and D. Galetti, *Phys. Rev. Lett.* **79**, 5218 (1997).
- [42] L. C. Chamon, B. V. Carlson, L. R. Gasques, D. Pereira, C. De Conti, M. A. G. Alvarez, M. S. Hussein, M. A. Cândido Ribeiro, E. S. Rossi, and C. P. Silva, *Phys. Rev. C* **66**, 014610 (2002).
- [43] D. Pereira, J. Lubian, J. R. B. Oliveira, D. P. de Sousa, and L. C. Chamon, *Phys. Lett. B* **670**, 330 (2009).
- [44] D. P. Sousa, D. Pereira, J. Lubian, L. C. Chamon, J. R. B. Oliveira, E. S. Rossi, C. P. Silva, P. N. de Faria, V. Guimarães, R. Lichtenthaler *et al.*, *Nucl. Phys. A* **836**, 1 (2010).
- [45] R. S. Mackintosh and N. Keeley, *Phys. Rev. C* **79**, 014611 (2009).
- [46] H. Kumawat, V. Jha, B. J. Roy, V. V. Parkar, S. Santra, V. Kumar, D. Dutta, P. Shukla, L. M. Pant, A. K. Mohanty, R. K. Choudhury, and S. Kailas, *Phys. Rev. C* **78**, 044617 (2008).
- [47] V. V. Parkar, I. Martel, A. M. Sánchez-Benítez, L. Acosta, K. Rusek, Ł. Standlyo, and N. Keeley, *Acta Phys. Pol. B* **42**, 761 (2011).
- [48] S. Santra, S. Kailas, K. Ramachandran, V. V. Parkar, V. Jha, B. J. Roy, and P. Shukla, *Phys. Rev. C* **83**, 034616 (2011).
- [49] V. V. Parkar, V. Jha, S. K. Pandit, S. Santra, and S. Kailas, *Phys. Rev. C* **87**, 034602 (2013).
- [50] L. R. Gasques, M. Dasgupta, D. J. Hinde, T. Peatey, A. Diaz-Torres, and J. O. Newton, *Phys. Rev. C* **74**, 064615 (2006).
- [51] V. V. Parkar, V. Jha, B. J. Roy, S. Santra, K. Ramachandran, A. Shrivastava, A. Chatterjee, S. R. Jain, A. K. Jain, and S. Kailas, *Phys. Rev. C* **78**, 021601(R) (2008).
- [52] V. Jha and S. Kailas, *Phys. Rev. C* **80**, 034607 (2009).
- [53] B. Buck and A. Merchant, *J. Phys. G: Nucl. Part. Phys.* **14**, L211 (1988).
- [54] C. R. Bingham and D. L. Hillis, *Phys. Rev. C* **8**, 729 (1973).
- [55] D. G. Fleming, *Can. J. Phys.* **60**, 428 (1982).
- [56] A. Kundu, S. Santra, A. Pal, D. Chattopadhyay, R. Tripathi, B. J. Roy, T. N. Nag, B. K. Nayak, A. Saxena, and S. Kailas, *Phys. Rev. C* **95**, 034615 (2017).
- [57] V. A. B. Zagatto, J. Lubian, L. R. Gasques, M. A. G. Alvarez, L. C. Chamon, J. R. B. Oliveira, J. A. Alcántara-Núñez, N. H. Medina, V. Scarduelli, A. Freitas, I. Padron, E. S. Rossi, Jr., and J. M. B. Shorto, *Phys. Rev. C* **95**, 064614 (2017).
- [58] A. Kundu, S. Santra, A. Pal, D. Chattopadhyay, R. Tripathi, B. J. Roy, T. N. Nag, B. K. Nayak, A. Saxena, and S. Kailas, *Phys. Rev. C* **99**, 034609 (2019).
- [59] K. Rusek, *Eur. Phys. J. A* **41**, 399 (2009).
- [60] I. J. Thompson, M. A. Nagarajan, J. S. Lilley, and M. J. Smithson, *Nucl. Phys. A* **505**, 84 (1989).
- [61] Y. Hirabayashi, S. Okabe, and Y. Sakuragi, *Phys. Lett. B* **221**, 227 (1989).
- [62] <https://www.nndc.bnl.gov/ensdf/>.
- [63] M. Dasgupta, P. R. S. Gomes, D. J. Hinde, S. B. Moraes, R. M. Anjos, A. C. Berriman, R. D. Butt, N. Carlin, J. Lubian, C. R. Morton, J. Newton, and A. Szanto de Toledo, *Phys. Rev. C* **70**, 024606 (2004).
- [64] C. Y. Wong, *Phys. Rev. Lett.* **31**, 766 (1973).
- [65] K. Rusek, N. Alamanos, N. Keeley, V. Lapoux, and A. Pakou, *Phys. Rev. C* **70**, 014603 (2004).